

1 **Modeling Pavement Noise with Different Tire Configurations using Coupled**
2 **FEM/BEM Analysis**

3
4 Hao Wang (Corresponding author)

5 Assistant Professor

6 Department of Civil and Environmental Engineering,

7 Rutgers, The State University of New Jersey

8 96 Frelinghuysen Road, Piscataway, NJ, 08854

9 848-445-2874

10 hwang.cee@rutgers.edu

11
12 Yangmin Ding

13 Graduate Research Assistant

14 Department of Civil and Environmental Engineering,

15 Rutgers, The State University of New Jersey

16 97 Frelinghuysen Road, Piscataway, NJ, 08854

17 yangmin.ding@rutgers.edu

18
19
20
21
22
23
24
25
26
27
28
29
30 Word Count: 4,500 + 10 figures and tables (2500) = 7000

31

1 **ABSTRACT**

2 This paper aims to predict tire-pavement interaction noise using a coupled finite element
3 modeling (FEM) and boundary element modeling (BEM) approach. A dynamic tire-
4 pavement interaction model was first developed using the FEM to obtain tire vibration
5 under harmonic excitations. The FEM simulation results provide the tire acceleration
6 histories that serve as the boundary condition for predicting the exterior acoustic field of
7 tire using the BEM. The developed FEM/BEM model was used to study the impact of
8 dual tires and wide-base tires on pavement noise. Two radial truck tires (275/80R22.5
9 and 445/50R22.5) were modeled and the tire models were validated with tire deflections
10 and contact stresses at the tire-pavement interface. The predicted contact stresses show
11 different non-uniform distribution patterns between the dual-tire assembly and the wide-
12 base 445 tire. Results indicate that the wide-base 445 tire was quieter than the dual tires
13 and the differences in A-weighted sound pressure levels were observed up to 8.6 decibels
14 (dB). The results illustrate the potential of using the developed model to capture the
15 influence of tire types or tire dimensions on tire-pavement interaction noise.

16
17
18

1 INTRODUCTION

2 In recent years, the trucking industry has developed innovations of tire technology for
3 purposes of improving the efficiency of vehicle operations and fuel consumption while
4 minimizing tire wear. An increased interest in the use of wide-base single tires as an
5 alternative to conventional dual-tire assemblies has occurred parallel to the recent interest
6 as an innovative tire technology. Historically, dual-tire assemblies have been used to
7 provide the largest footprint to adequately distribute the axle load onto the pavement
8 surface. However, compared to conventional dual-tire assembly, wide-base tires has the
9 potential to offer several benefits, including improved fuel efficiency, increased hauling
10 capacity, reduced wheel cost, and superior ride and comfort (1).

11 The effects of wide-base tires on the road infrastructure is receiving considerable
12 attention and eliciting widespread interest in pavement researchers, particularly since the
13 introduction of new generation of wide-base tires (wide-base 445 and 455) in 2000s. The
14 impact of the new generation of wide-base tires on pavement damage was firstly
15 investigated in 2000. A comprehensive study was conducted to compare the pavement
16 responses under wide-base tires and the dual-tire assembly on the heavily instrumented
17 Virginia Smart Road. A number of studies were conducted to investigate the pavement
18 damage mechanisms induced by different tire configurations using theoretical modeling
19 and field instrumentations. These studies concluded that the new wide-base 445 or 455
20 tire could cause greater or less pavement damage potential than the dual-tire assembly,
21 depending on the pavement structure and failure mechanism (2-6).

22 The aforementioned studies focus on the impact of wide-base tires on pavement
23 damage. However, researches on the impact of wide-base tires on environment,
24 especially the influence on tire-pavement noise is quite limited. Noise, defined as
25 unwanted or excessive sound, has become one of the greatest sources of nuisance and
26 environmental exposures in the United States (7). While noise emanates from different
27 sources, traffic noise is perhaps the most pervasive and difficult source to avoid (8). In
28 1981, the U.S. Environmental Protection Agency (EPA) estimated that approximately
29 100 million people (about 50% of the population) in the United States had annual
30 exposures to traffic noise that were high enough to threaten the health (9).

31 Traditionally, traffic noise is related with exhaust and engine noise of vehicles. With
32 the development of automobile technology, the emission and propagation noise from
33 such sources are greatly controlled. Instead, the tire-pavement interaction noise becomes
34 dominant. As a major component of the vibrating source of the tire-pavement noise, the
35 tire plays a significant role in noise control (10). The literature survey shows that most
36 researchers consider the effect of tire dimensions on tire-road noise via the use of large-
37 scale field or laboratory tests (11). These test methods consume considerable manpower,
38 materials and financial resources. The testing results are susceptible to the interference
39 from a variety of factors, such as environmental factors, traffic conditions, etc. Hence, it
40 is desired to develop a numerical simulation method for evaluating the impact of new
41 generation wide-base tire on tire-pavement noise, as an important means of developing
42 wide-base tire.

43 OBJECTIVE AND SCOPE

44 This study explores the application of a modeling approach to predict tire-pavement noise
45 level with different tire configurations. A coupled BEM/FEM analysis approach was
46

1 developed for prediction of tire-pavement interaction noise. Initially, a radial truck tire
2 was first built using the FEM and the surface accelerations under harmonic excitations
3 were obtained from the modal analysis. Then the solutions for the radiation sound fields
4 caused by the tire vibration were solved using the BEM analysis. The tire model was
5 validated with tire deflection and contact stresses at the tire-pavement interface. The
6 FEM/BEM model was used to predict the sound pressure level generated by two truck
7 tire configurations (275/80R22.5 and 445/50R22.5) on the porous asphalt concrete (PAC).
8 Numerical predictions were compared with existing experimental observations from
9 literature and showed consistent trends.

11 **SIMULATION OF TIRE VIBRATION RESPONSES**

12 To apply a tire model to tire-pavement interaction noise prediction, a model needs to be
13 efficient yet accurately represents the tire structure behavior. Modern tires are structurally
14 complicated, consisting of layers of belts, plies, and bead steel imbedded in rubber. The
15 tire industry developed plentiful simplified models to predict tire performance, among
16 which are the classical spring-damper model, the tire ring model and the membrane and
17 shell model (12). Among numerous notable published contributions to tire modeling are
18 publications by Pottinger and Joseph (13-14). Ahmad (15) developed a non-linear finite
19 element model of the interaction of a tractor tire with soil surface for analyzing the
20 contact pressure distribution for varying load conditions. Models commonly used for tire
21 design purposes can accurately simulate tire performance, and the interaction of internal
22 components. However, such models are extremely large and require long computing time.
23 Besides, the tire material properties and related modeling details for tire models used by
24 the industry are extremely difficult to obtain. Since the concern in this paper focuses on
25 the deformation as it relates to the contact area and its ability to obtain modal
26 characteristics, a simpler model can be employed for better computational efficiency.

28 **Descriptions of Tire Finite Element Model**

29 In this paper, two truck radial tires (275/80R22.5 and 445/50R22.5) were built under the
30 same inflation pressure 724kPa, with load of 17.8kN and 35.6kN respectively, and a
31 friction coefficient of 0.55. The nomenclature of tires usually includes three tire
32 dimensions and types of tire in the form of AAA/BBXCC.C (16). The first number (AAA)
33 is the tire width from wall to wall in mm or inch, the second number (BB) is the sidewall
34 height given as a percentage of the tire width. The letter (X) indicates the type of tire
35 (radial or bias ply). The third number (CC.C) is the tire rim diameter in inches. For
36 example, a tire designation 445/50R22.5 is a radial tire (indicated with the "R"), with a
37 wall-to wall width of 445mm, a wall height of 222.5mm, and a rim diameter of 22.5in
38 (571.5mm). The two tire configurations (17), single wide-base and standard dual, are
39 shown together in Figure 1.

40 Previous studies have pointed out that a tire model should consider the following main
41 characteristics: 1) the composite material and the anisotropy resulted from the stiffness
42 difference between rubber and reinforcement; 2) the relatively large deformation due to
43 flexibility of tire carcass during tire pavement interaction; and 3) the nearly-
44 incompressible and nonlinearity of rubber (18). The choice of material model depends on
45 balancing the type of behavior desired in the model with the information available to
46 determine tire model parameters. The tread and sidewalls are constructed from rubber,

1 and the belts and carcass are made of fiber-reinforced rubber composites. Both the rubber
2 and fiber reinforcement are modeled as linear elastic material. Generally, the tire
3 simulation consists of mounting the tire on the rim, followed by inflating it, lowering the
4 tire onto a non-deformable surface, and applying various loading conditions.
5



6
7 **FIGURE 1. Wide-base single (445/50R22.5) and on tire of dual-tire assemblies**
8 **(275/80R22.5).**
9

10 The simulation of FE tire model in this study includes three steps. In the first step, an
11 internal inflation pressure is applied on the axisymmetric tire model. The second step of
12 the simulation is generation of a full three-dimensional tire model by using the symmetric
13 results transfer and symmetric model generation (19). In the last step the static deformed
14 shape of the pressurized tire under a vertical load was modeled. The road surface is
15 modelled as analytical rigid body. Two-dimensional tire mesh and three-dimensional tire
16 mesh are shown in Figure 2.

17 The contact between the tire and pavement surface consists of two components: one
18 normal to the surfaces and one tangential to the surfaces. The treatment of the normal
19 contact condition is to enforce impenetrability in the normal direction using the penalty
20 method or Lagrange multipliers method. However, for the tangential interaction between
21 two contacting surfaces, the typical Coulomb friction law is used. This model assumes
22 the resistance to movement is proportional to the normal stress at an interface. In this case,
23 the interface may resist movement up to a certain level; then the two contacting surfaces
24 at the interface start to slide relative to each another. If the relative motion occurs, the
25 frictional stress remains constant and the stress magnitude is equal to the normal stress at
26 the interface multiplied by the friction coefficient.
27

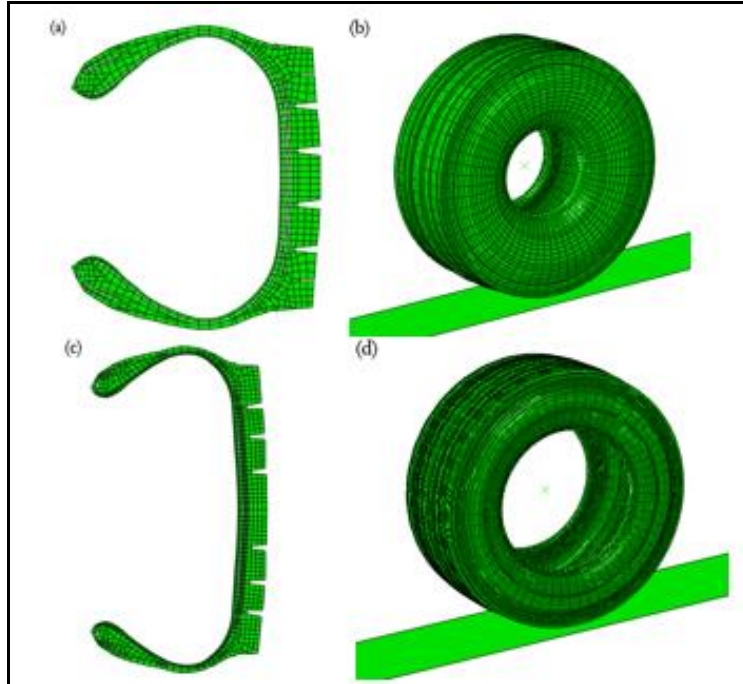
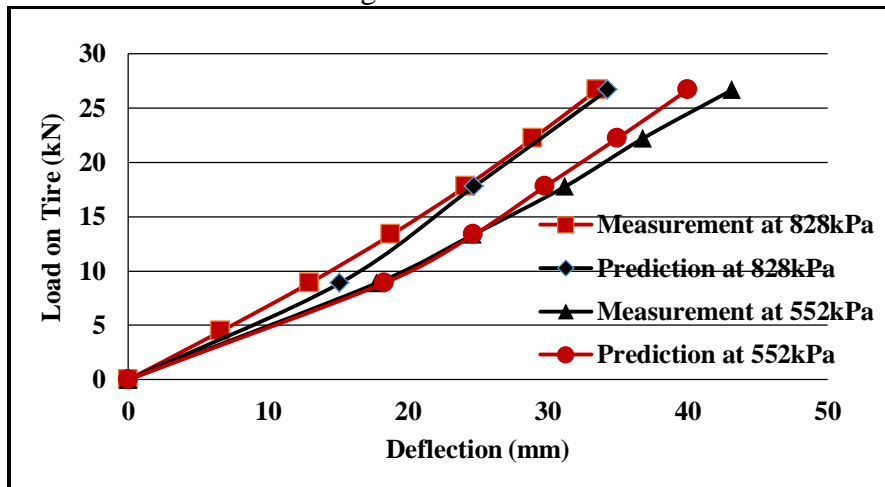


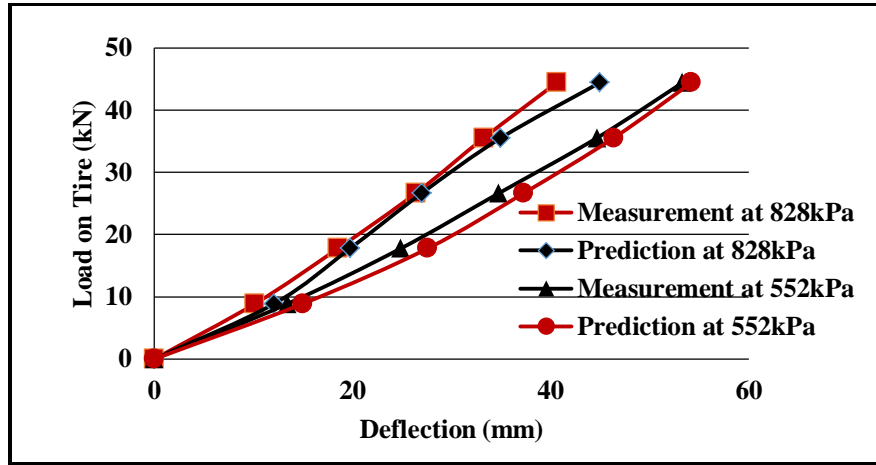
FIGURE 2. Tire finite element meshes (a) Two-dimensional 275 tire mesh; (b) Three-dimensional 275 tire mesh (c);Two-dimensional 445 tire mesh; (d) Three-dimensional 445 tire mesh.

Validation of Tire Finite Element Model

Tire deflection is an important measure of the tire stiffness in response to the vertical load. In this paper, tire load deflection curves and measured contact stresses curves from experimental measurements are used to calibrate the tire model (20, 21). Good agreements were achieved between the calculated tire deflections and measurements under different load and pressure conditions, as illustrated in Figure 3. A mesh sensitivity analysis with a series of gradually finer finite element meshes was conducted to refine the mesh in the contact area. By comparing the predicted contact stresses for each mesh, the final mesh was selected until the changes in the result was smaller than 5%.



(a)

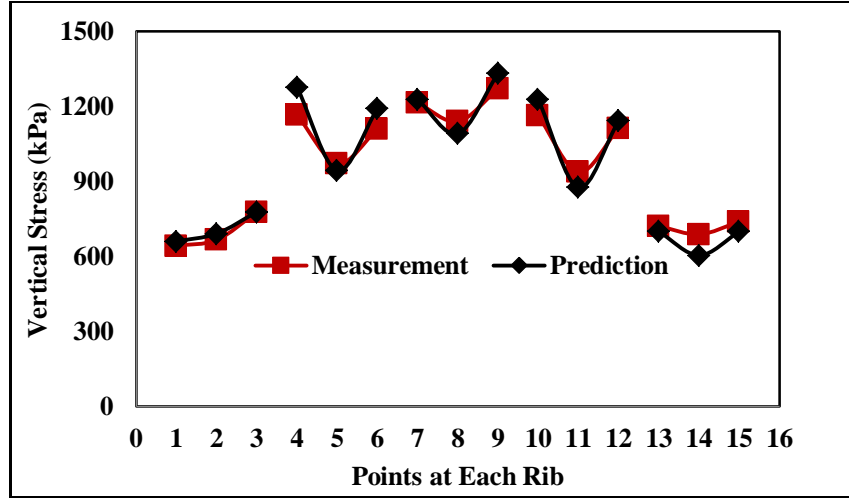


(b)

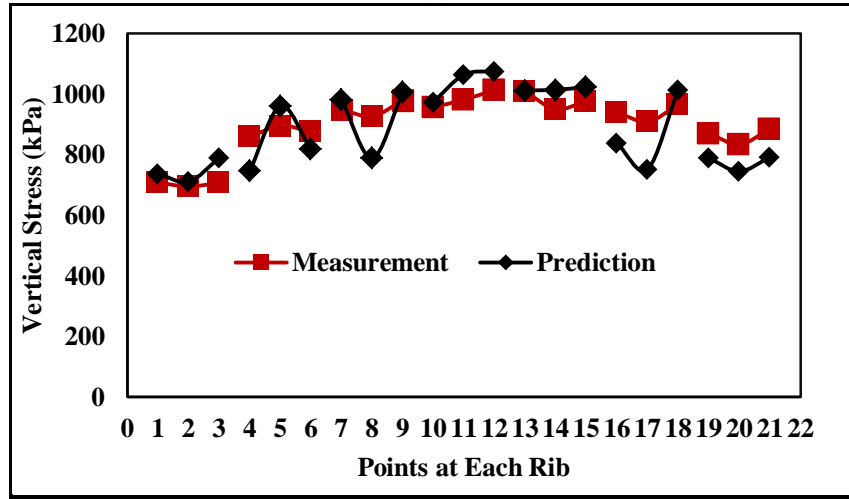
FIGURE 3. Comparisons between measured and predicted deflections for (a) dual 275 tire and (b) wide-base 445 tire.

The predicted vertical contact stresses at the tire-pavement contact zone were compared to the experimental measurements provided by the tire manufacturer. As shown in Figure 4, the tire model captured the non-uniform distribution of vertical contact stresses under each individual tire rib. As the tire is pressed against a flat surface, the tread rubber is compressed in the flattened contact patch and the sidewall of the tire is in tension. The bending stress in the sidewall causes the non-uniform distribution of vertical contact stresses in the contact patch, particularly at the edge of the contact patch. The maximum vertical stress under the center rib was found to be 1.4-1.6 times the inflation pressure owing to the non-uniform contact stress distribution.

The results indicate that the wide-base tire has relatively more uniform vertical stress distribution along the tire width compared to the dual-tire assembly, which is consistent with the measurements reported in the authors' previous work (4). It is noted that the non-uniform contact stresses have significant influence on pavement responses at the near-surface, as indicated in the previous work by the authors (5, 6). Based on the good agreement in the measured tire deflections and contact stresses, the proposed tire model is assumed to be reasonable for tire-pavement interaction analysis.



(a)



(b)

FIGURE 4. Comparisons between measured and predicted vertical contact stress for (a) dual tires and (b) wide-base tire.

Tire Modal Shapes and Vibration Responses

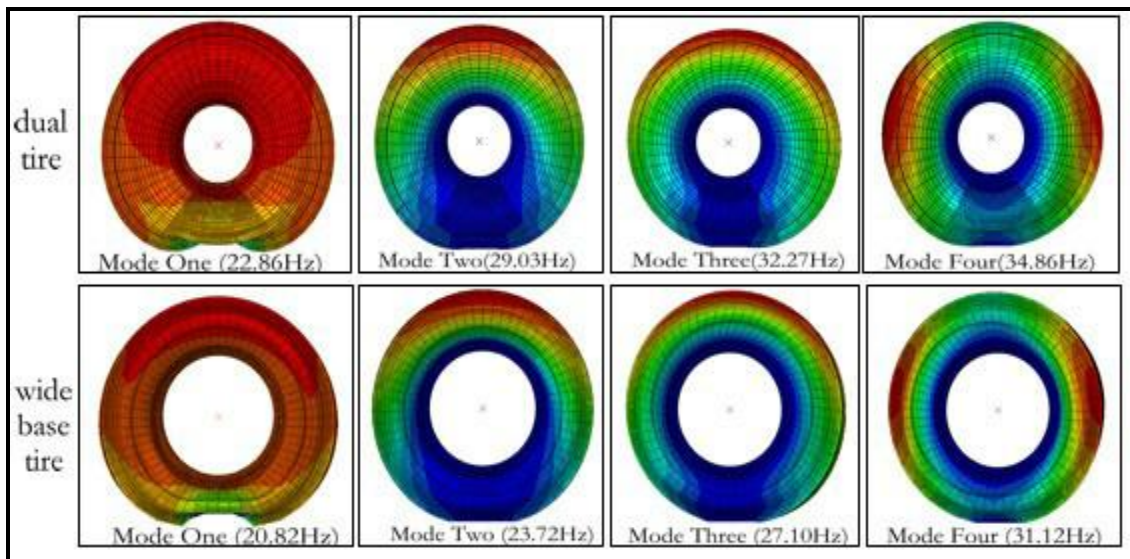
Modal analysis was conducted to identify the natural frequencies and mode shapes of the tire. The BEM requires a tire geometry and the surface acceleration to predict the acoustic pressure and intensity. The surface acceleration is obtained from the modal characteristics of a tire under harmonic excitation. The eigenvalue problem for natural modes of small vibration of a FEM model is shown in Equation 1.

$$(u^2[M] + u[C] + [K])\{\phi\} = 0 \quad (1)$$

where, $[M]$ is the mass matrix; $[C]$ is the damping matrix; $[K]$ is the stiffness matrix; u is the eigenvalue; and $\{\phi\}$ is the eigenvector, the mode of vibration. Typically, for symmetric eigenproblems, $[K]$ is assumed positive semidefinite. In this case u becomes an imaginary eigenvalue, $u = iw$ where w is the circular frequency and the eigenvalue problem can be simplified as Equation 2.

$$(-w^2[M] + [K])\{\phi\} = 0 \quad (2)$$

1 Two approaches can be used for solving the symmetrized eigenproblems: subspace
 2 iteration method and Lanczos method. Both methods use the Householder and Q-R
 3 algorithm for the reduced eigenproblem. The basic idea of the subspace iteration method
 4 is simultaneous inverse power iteration. In this method, a small set of base vectors is
 5 generated, which defines a “subspace”. Then the “subspace” is transformed, by iteration,
 6 into the space containing the lowest few eigenvectors of the overall system (22). The
 7 Lanczos procedure consists of a set of Lanczos “runs”, in each of which a set of steps is
 8 performed. The Lanczos eigensolver is a powerful tool for extraction of the extreme
 9 eigenvalues and the corresponding eigenvectors of a sparse symmetric generalized
 10 eigenproblem (23). This paper employs Lanczos method for tire modal analysis. There
 11 were a total of 20 structural vibration modes identified from the FEM modal analysis in
 12 the frequency range between 10-800 Hz. Figure 5 illustrates the first four radial modes of
 13 tire vibration, respectively, for one tire in dual-tire assembly and the wide-base 445 tire.
 14



15
 16 **FIGURE 5. Finite element modal analysis results.**
 17

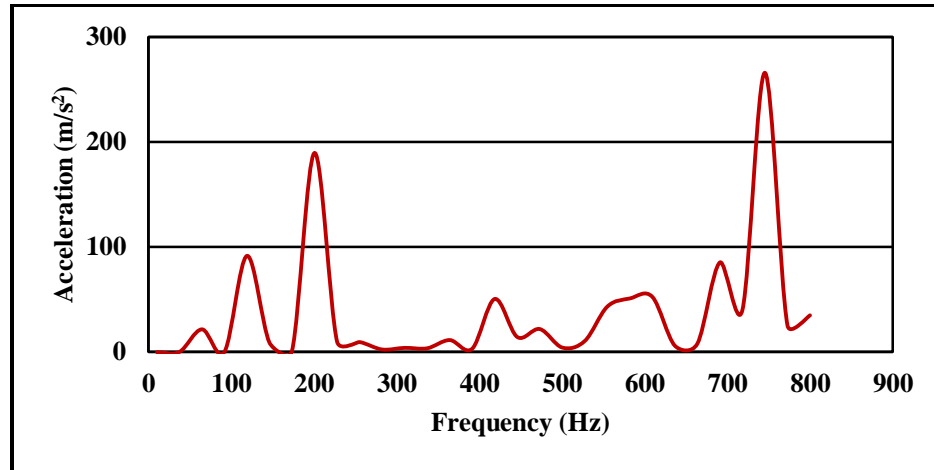
18 Steady state linear dynamic analysis predicts the linear response of a structure
 19 subjected to continuous harmonic excitation. The set of eigenmodes extracted in the
 20 previous eigenfrequency step were used to calculate the steady state solution as a
 21 function of the frequency of the applied excitation. The structural dynamics equation for
 22 steady-state response under a harmonic excitation is shown in Equation 3.

$$23 \quad ([K] + iw[C] - w^2[M])\{U\} = \{F\} \quad (3)$$

24 where, $\{U\}$ is the nodal displacement vector of the structure; and $\{F\}$ is the load vector of
 25 the external excitation.

26 The acceleration response obtained in the FE analysis was used as a boundary
 27 condition for a BEM analysis of the transmitted noise field. Generally, tire-pavement
 28 noise can be described as two mechanisms: the mechanical vibrations of the tire, and the
 29 aerodynamic phenomenon (10). In this study, only the vibrations noise is taken into
 30 consideration. Since the frequency spectrum characteristic of noise is not affected by the
 31 amplitude of the harmonic excitation, the acceleration responses of the tire was calculated
 32 with harmonic point loads of unit magnitude in the frequency range from 10 to 800Hz.

1 The point load is applied to the analytical rigid surface through its reference node. Figure
 2 6 illustrates the acceleration frequency response of a node from the tire sidewall.
 3



4
 5 **FIGURE 6. Example of tire acceleration spectrum at 37.24Hz for one tire in dual-**
 6 **tire assembly**

8 TIRE-PAVEMENT NOISE PREDICTION

10 Basic Theory of BEM

11 The mathematical formulation and practical application of the BEM have been discussed
 12 in details in previous publications, such as Brebbia and Walker (24), Telles and Wrobel
 13 (25). The application of the BEM to wave problems can be found in the work of Shaw
 14 and Copley (26, 27).

15 As a numerical method used to solve a wide variety of boundary value problems, there
 16 are two approaches in the boundary element formulation: the direct boundary element
 17 method (DBEM) and the indirect boundary element method (IBEM). In the DBEM the
 18 physical variables, such as acoustical pressure and acoustical velocity are solved directly
 19 from the discretized surface integral equations. By comparison, in the IBEM the problem
 20 is formed in accordance with a source density function, and the distribution of fictitious
 21 sources is solved on the boundary. In this study, only the DBEM was used.

22 The governing partial differential equation for linear acoustics in the frequency domain
 23 is the Helmholtz equation, Equation 4.

$$24 \quad (\nabla^2 + k^2)p = 0 \quad (4)$$

25 where, ∇^2 is the Laplace operator and p is the acoustic pressure. $k = w/c$ is the wave
 26 number. w is the angular frequency and c is the speed of sound. The boundary condition
 27 for the vibro-acoustic problems is given in Equation 5.

$$28 \quad \partial p / \partial n = -i\rho w v_n \quad (5)$$

29 where, n is the normal vector pointing outside from the acoustic volume; $i = \sqrt{-1}$ is the
 30 imaginary unit; ρ is the acoustic fluid density and v_n is the normal velocity. From the
 31 theory of Green's functions, Equation 6 can be recast into the Helmholtz integral for an
 32 exterior boundary value problem (28):

$$p(P) = \int_{\Gamma} \left(G \frac{\partial p}{\partial n} - p \frac{\partial G}{\partial n} \right) d\Gamma \quad (6)$$

where, $G = e^{-ikr} / 4\pi r$ is the singular fundamental solution, and r is the distance between the field point.

Boundary Element Modeling of Tire Pavement System

The acceleration response obtained in the FE analysis as described in the previous section is used as a boundary condition for a BEM analysis of the transmitted noise field. To solve the acoustic problem, the DBEM formulation was used in this study. For a given acceleration field on the tire BEM surface, an acoustic BEM direct frequency response analysis calculates pressure and normal acceleration values at all the boundary nodes and field points. The outer surface elements of the tire were selected to constitute the boundary element. In order to avoid sound leakage, additional elements were added to the rim. In the dual-tire model, a symmetric total reflection panel is built to simulate the other tire. The distance between the symmetric panel and tire is 310 mm (dual spacing). The boundary of the BE model is exactly the same as the FE model of the tire, in this way the acceleration response of the tire could be transferred directly to the BE model.

Tire-Pavement Noise under Different Tire Configurations

In this study, field points to calculate sound pressure are chosen to be identical to the measurement location in the CPX method. Instead of measuring sound intensity level from a phase-matched pair of microphones (as the OBSI method does), CPX measures levels via sound pressure from a single microphone. According to the ISO/DIS 11819-2, the microphone positions in the CPX method are illustrated in Figure 7. The five microphones in CPX method are modeled with corresponding five field points in BEM. Table 1 presents the exact positions of the field points in BEM. The coordinates of the origin is (0, 0, 0) located at the tire center.

TABLE 1 Field point coordinates for dual-tires and wide-base tire

Field Point	X Coordinate (mm)	Y Coordinate (mm)	Z Coordinate (mm)
Dual Tires			
1	0	337	265
2	200	337	265
3	-200	337	265
4	650	0	165
5	-650	0	165
Wide-base Tire			
1*	0	422	435
2*	200	422	435
3*	-200	422	435
4*	650	0	335
5*	-650	0	335

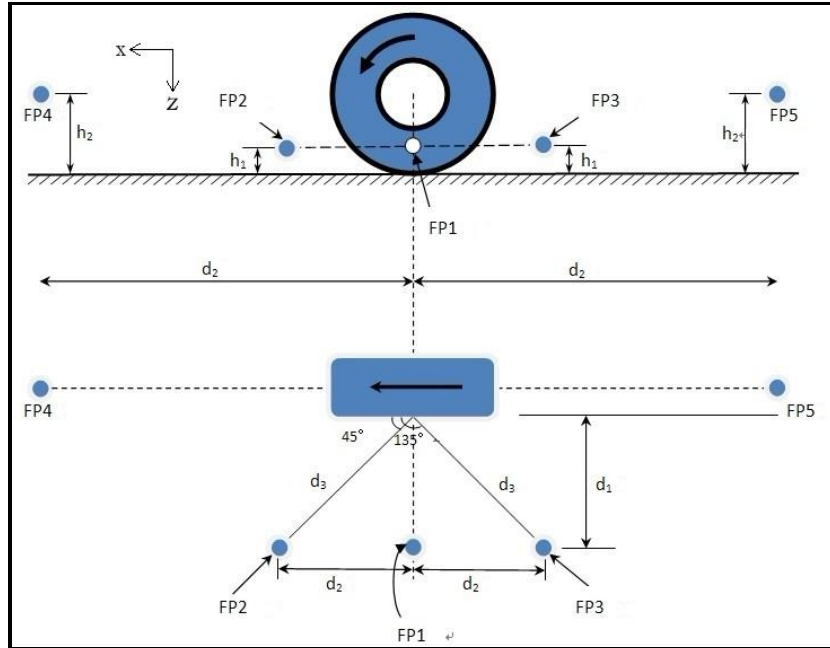


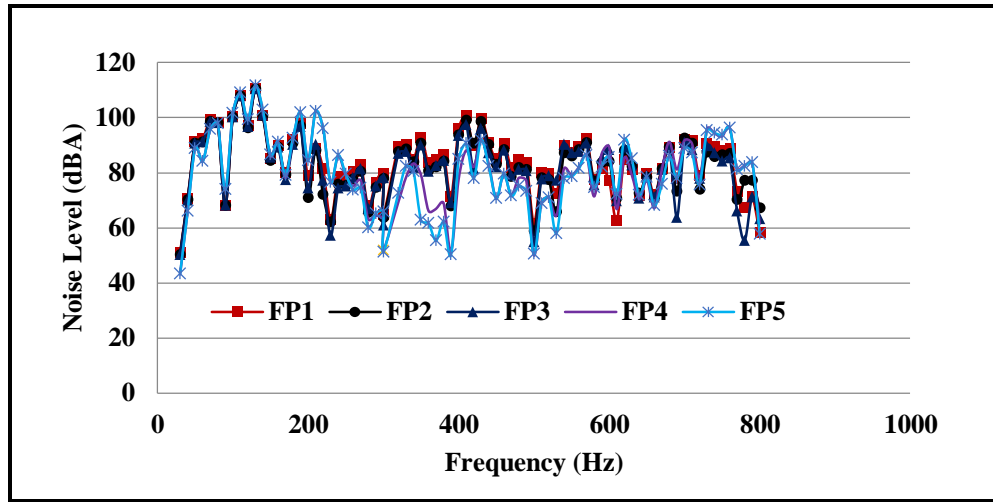
FIGURE 7. Microphone positions in the CPX method.

1
2
3
4 The road surface in the BEM was modeled as porous asphalt concrete (PAC) surfaces.
5 PAC consists primarily of gap-graded aggregates held together by a polymer modified
6 binder to form a matrix with inter-connecting voids. Unlike conventional asphalt
7 pavements, PAC typically possesses 15-25 % void volume (11). In effect this increase in
8 porosity means that the PAC acts as porous sound-absorbent materials and greatly
9 absorbs the sound, converting it into a small amount of friction energy, thereby reducing
10 noise. To theoretically model the sound propagation through a porous absorber, it is
11 necessary to have frequency dependent sound velocity, and frequency dependent mass
12 density which characterize the acoustic properties of the absorbent acoustic medium. In
13 our previous work, a theoretical model has been developed to analyze the effects of pore
14 structure parameters (pore radius, pore length and porosity) on the acoustic absorption
15 coefficient of PAC. The porous material parameters with pore radius 6mm, pore length
16 4cm and porosity 25% used in this study are obtained from our previous work (29).

17 Figures 8 (a) and (b) illustrate the frequency responses of the sound pressure level at
18 the field points, respectively, for the dual-tire assemble and the wide-base tire. In the
19 figures, there are several dominant peaks of sound pressure responses at different
20 frequencies. The simulated tire-pavement noise peak is higher than the present
21 experimental data and the trend of the noise level curves have more fluctuations
22 compared to the measured data from existing literatures (30-31). That may be partly
23 attributed to the effects of the simple harmonic excitation and factors related to tire
24 parameters like tire material, tire dimension. Other factors like temperatures and the
25 rolling condition of tire could also affect the noise level.

26 It was observed from the figures that the wide-base tire induces smaller sound pressure
27 level at the low frequency range (10-200Hz). While within the frequency range higher
28 than 200Hz, the wide-base tire causes the same noise level compared with the
29 conventional dual tires. This probably because the acceleration response difference
30 between these two tires as discussed in the above section.

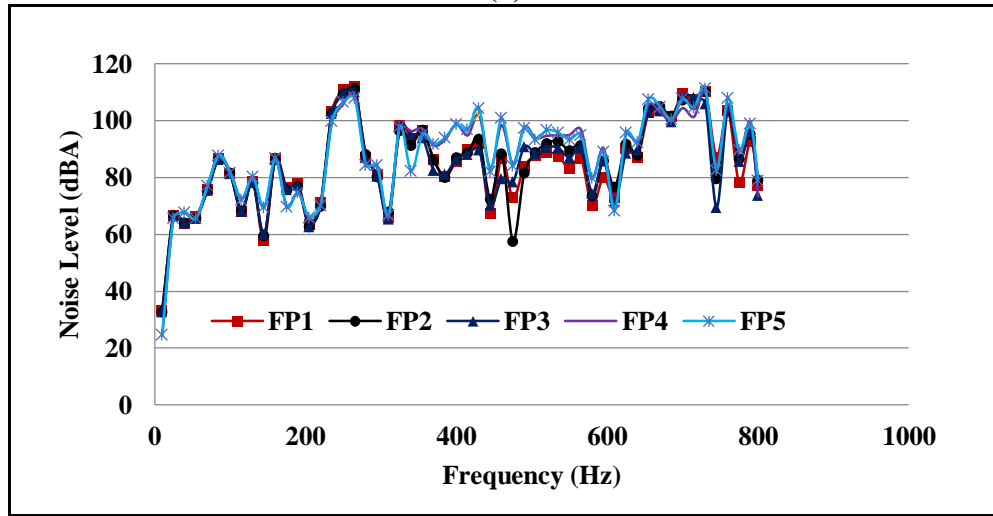
1



2

3

(a)



4

5

(b)

6

FIGURE 8. Sound pressure at selected field points for (a) dual-tire assembly and (b) wide-base tire.

7

8

9

The analysis in Figure 8 simulates sound pressure level at different frequency bands L_{pi} . The overall sound pressure level L_p is calculated as

10

11

$$L_p = 10 * \log_{10} \sum_{i=1}^N 10^{L_{pi}/10} \quad (7)$$

12

TABLE 2 Comparison of overall noise level at field points

Tire Type	FP1 (dBA)	FP2 (dBA)	FP3 (dBA)	FP4 (dBA)	FP5 (dBA)
Dual-tire assemblies	125.5	125.1	125.0	126.4	126.4
Wide-base tire	118.2	117.5	117.0	116.7	117.8

13

14

15

The overall noise levels for these two kinds of tires at field points are presented in Table 2. Concerning the impact of wide-base tire and dual tires on overall tire pavement interaction noise level, it has been shown here that the wide-base tires is quieter than the

1 dual tires. Differences in A-weighted sound pressure levels up to 8.6 dB(A) are observed.
2 One possible reason why dual-tires seem to emit higher noise levels may be that the
3 number of tires is higher. As literature (11) showing 16 wheels of a typical tractor-
4 semitrailer combination give 6 dB higher noise level than a reference four-wheel vehicle.
5 Further investigation is needed to validate the finding using field noise measurements for
6 different truck tires.

8 CONCLUSIONS

9 In this study, a coupled FEM and BEM model was developed to predict tire-pavement
10 interaction noise. The results show that the sound field caused by tire vibration and
11 absorption properties of pavement surface can be predicted with appropriate selection of
12 the excitation spectrum and acoustic parameters of pavement surface using the developed
13 approach. The FEM/BEM model was used to predict the noise generated by the two truck
14 radial tires. The results show that in the low frequency range lower than 200Hz, the dual-
15 tire assembly is noisier than the wide-base tire. However, within the frequency range
16 higher than 200Hz, the wide-base tire causes the similar noise level compared to the
17 conventional dual tires. Concerning the impact of tire configuration on the overall tire-
18 pavement interaction noise, it was found that the new generations of wide-base tire is
19 quieter than the dual tires. Differences in A-weighted sound pressure levels were
20 observed up to 8.6 dB(A). The results illustrate the potential of using the developed
21 model to capture the influence of tire types or tire dimensions on tire-pavement
22 interaction noise.

24 REFERENCES

- 25 1. Al-Qadi, I. L., and M. A. Elseifi. New Generation of Wide-Base Tires: Impact on
26 Trucking Operations, Environment, and Pavements. In *Transportation Research*
27 *Record: Journal of the Transportation Research Board*, No. 2008, Transportation
28 Research Board of the National Academies, Washington, D.C., 2007, pp. 100-109.
- 29 2. Al-Qadi, I. L., A. Loulizi, I. Janajreh and T.E. Freeman. Pavement Response to Dual
30 Tires and New Wide-Base Tires at Same Tire Pressure. In *Transportation Research*
31 *Record: Journal of the Transportation Research Board*, No. 1806, Transportation
32 Research Board of the National Academies, Washington, D.C., 2002, pp. 38-47.
- 33 3. Greene, J., U. Toros, S. Kim, T. Byron., and B. Choubane. (2010) Impact of Wide-
34 Base Tires on Pavement Damage. In *Transportation Research Record: Journal of the*
35 *Transportation Research Board*, No. 2115, Transportation Research Board of the
36 National Academies, Washington, D.C., 2010, pp. 82-90.
- 37 4. Wang, H. and I.L. Al-Qadi, Impact Quantification of Wide-base Tire Loading on
38 Secondary Road Flexible Pavements, *Journal of Transportation Engineering*, Vol.
39 137. No.9, ASCE, 2011, pp. 630-639.
- 40 5. Al-Qadi, I.L., and H. Wang, Impact of Wide-Base Tires on Pavements: Results from
41 Instrumentation Measurements and Modeling Analysis, In *Transportation Research*
42 *Record: Journal of the Transportation Research Board*, No. 2304, TRB, 2012, pp.
43 169-176.
- 44 6. Wang, H. and I.L. Al-Qadi, Combined Effect of Moving Wheel Loading and Three-
45 Dimensional Contact Stresses on Perpetual Pavement Responses, In *Transportation*

- 1 *Research Record: Journal of the Transportation Research Board*, No. 2095, TRB,
2 2009, pp. 53-61.
- 3 7. Garc á A. *Environmental Urban Noise*, Wentworth Insitute of Technology Press,
4 Boston, 2001.
- 5 8. Mark, F. *Highway Traffic Noise in the United States-Problem and Response*,
6 Publication FHWA-HEP-06-020. FHWA, U.S. Department of Transportation, 2006.
- 7 9. Simpson, M., and R. Bruce. *Noise in America: Extent of the Noise Problem*, Report
8 550/9-81-101. Washington, DC, Environmental Protection Agency, 1981.
- 9 10. Hanson, D. I., R. S. James, and C. NeSmith. *Tire/Pavement Noise Study*. Report 04-
10 02. Auburn, National Center for Asphalt Technology, 2004.
- 11 11. Sandberg U., J. A. Easement. *Tire/Road Noise Reference Book*. Informex, Kisa, 2002.
- 12 12. Knothe, K. Advanced Contact Mechanics-Road and Rail, *Vehicle System Dynamics*,
13 Vol. 35, 2001, pp. 361-407.
- 14 13. Pottinger, M. G. Three-Dimensional Contact Patch Stress Field of Solid and
15 Pneumatic Tires. *Tire Science and Technology*, Vol. 20, 1992, pp. 3-32.
- 16 14. Padovan, J. On Standing Waves in" Tires". *Tire Science and Technology*, Vol. 5,
17 1997, pp. 83-101.
- 18 15. Ahmad M. Modelling of Pneumatic Tractor Tire Interaction with Multi-Layered Soil.
19 *Biosystems Engineering*, Vol. 104, 2009, pp. 191-198.
- 20 16. Wang, H. *Analysis of Tire-Pavement Interaction and Pavement Responses Using a*
21 *Decoupled Modeling Approach*. Ph.D. Dissertation, University of Illinois at Urbana-
22 Champaign, Illinois, USA, 2011.
- 23 17. Angela L. P., H. David and E. B. William. *Mechanistic Comparison of Wide-base*
24 *Single Vs. Standard Dual Tire Configurations*. NCAT Report 05-03, 2005.
- 25 18. Wong, J.Y. *Theory of Ground Vehicles*, John Wiley & Sons, Inc., New York, 1993.
- 26 19. *ABAQUS Analysis User's Manual*. Abaqus, Version 6.10-EF, 2010.
- 27 20. Hernandez, J.A., and A. Gamez, and I.L. Al-Qadi. Introducing an Analytical
28 Approach for Predicting 3D Tire-Pavement Contact Load. In *Transportation*
29 *Research Record: Journal of the Transportation Research Board*, No.14-2201, 2014.
- 30 21. Wang, H., I. L. Al-Qadi, and I. Stanciulescu. Simulation of Tire-Pavement Interaction
31 for Predicting Contact Stresses at Static and Various Rolling Conditions.
32 *International Journal of Pavement Engineering*, Vol. 12, 2012, pp. 310-321.
- 33 22. Ramaswami, S. *Towards Optimal Solution Techniques for Large Eigenproblems in*
34 *Structural Mechanics*, Ph.D. Thesis, MIT, 1979.
- 35 23. Parlett, B.N. Toward a Black Box Lanczos Program. *Computer Physics*
36 *Communications*, Vol. 53, 1989, pp. 169-179.
- 37 24. Brebbia, C.A., S. Walker. *Boundary Element Techniques in Engineering*. Newness-
38 Butterworths, 1980.
- 39 25. Brebbia, C. A., J. Telles, J, and L., Wroble. *Boundary Element Techniques: Theory*
40 *and Applications in Engineering*, Springer-Verlag, 1984.
- 41 26. Shaw, R. P. Boundary Integral Equation Methods Applied to Wave Problems.
42 *Applied Science Publishers*, Vol. 1, 1979, pp. 121-153.
- 43 27. Copley, L. G. Integral Equation Method for Radiation from Vibrating Bodies. *The*
44 *Journal of the Acoustical Society of America*, Vol. 41, 1967, pp. 807-816.
- 45 28. Wu, T.W. *Boundary element acoustics: Fundamentals and computer codes*. WIT
46 Press, United Kingdom, 2000.

- 1 29. Wang, H., Ding, Y. M., and Liao, G. Y. Modeling and Optimization of Acoustic
2 Absorption for Porous Asphalt Concrete. *Journal of Engineering Mechanics*, 2014
3 (Under Review).
- 4 30. McDaniel, R. S. Field Evaluation of Porous Friction Course for Noise Control.
5 Presented at 84th Annual Meeting of the Transportation Research Board, Washington,
6 D.C., 2005.
- 7 31. McDaniel, R. S. *Field Evaluation of Porous Asphalt Pavement*. Final Report, SQDH
8 2004-3. North Central Superpave Center, West Lafayette, Ind., 2004.